Tunnelling and Underground Space Technology 71 (2018) 478–493

Contents lists available at ScienceDirect

Tunnelling and Underground Space Technology

journal homepage: www.elsevier.com/locate/tust

Longitudinal deformation profile of a tunnel in weak rock mass by using the back analysis method

Yanbin Luo[a,*], Jianxun Chen[a,*], Yi Chen[b], Pengsheng Diao[a], Xiong Qiao[c]

[a] School of Highway, Chang'an University, Xi'an 710064, China
[b] China Guangzhou Metro Design & Research Institute Co., Ltd, Changsha 410000, China
[c] School of Civil Engineering, Lanzhou University of Technology, Lanzhou 730050, China

ARTICLE INFO

Keywords:
Weak rock mass tunnel
Longitudinal deformation profile (LDP)
Complete deformation
Displacement back analysis
Numerical simulation

ABSTRACT

Analysis of the rock mass deformation behavior is a very important aspect of the safety assessment for tunnel construction in weak rock mass. In this paper, the deformation characteristics of a soft rock mass tunnel using three beaches construction method were investigated, which include the crown settlement and horizontal displacement and have 9 sections with 3 different construction schemes. The optimized construction schemes by decreasing the beaches length and changing the geologist of primary support were proposed. Then, applying the displacement back analysis method to calculate the rock mass parameters, double parameters were analyzed by using the golden section method. Results show that the tunnel deformations were affected by the elastic modulus E and the lateral pressure coefficient λ of rock mass, and the change of E has greater influence than λ on the tunnel deformation. The change of λ has greater influence on the crown settlement than that on the horizontal displacement. Furthermore, the regularity and characteristics of longitudinal deformation profile (LDP) in a weak rock mass tunnel was studied by utilizing the Fast Lagrangian Analysis of Continua (FLAC), and the LDP of the three long-beach construction scheme and the three short-beach construction scheme were compared. The results show that the complete displacements of tunnel under the three short-beach construction scheme condition by decreasing the lengths of the middle and lower benches are smaller than that under the three short-beach construction scheme condition, however the pre-deformation of the tunnel deformation under this two construction scheme conditions is nearly the same. The extrusion deformation at the tunnel face of the three short-beach construction scheme is larger than that of the three long-beach construction scheme. Therefore, increasing the area of the core soil is a feasible measure to control the extrusion deformation on the tunnel face. Finally, the tunnel optimized construction scheme was verified benefit the tunnel stability. The measures of decreasing the length of middle and lower bench and closing the invert early and immediately will benefit the tunnel stability.

1. Introduction

By the end of 2015, 14006 highway tunnels with a total length of approximately 12,684 km have been constructed for operation in China. Recently, the construction speed of highway tunnels has exceeded 1000 km annually. China has been at the forefront of tunnel construction in terms of quantity, scale, and difficulty. Many tunnels are constructed in the weak rock mass, thereby resulting in complex engineering problems which are encountered by Chinese engineers. The most common engineering problems in tunnelling include large deformation, considerable clearance limit, and collapsing. The tunnel deformation behavior in weak rock mass is complex, therefore, the aforementioned engineering problems have occurred in various local and overseas tunnel constructions, such as the Tauern tunnel in Austria, Enasan tunnel in Japan, Jia Zhuqing tunnel of the Nanning to Kunming railway in China, and Wu Shaoling tunnel in Gansu province (China). These engineering problems could affect the speed and safety of construction, as well as cause the construction to go out of control, costly failure, and casualties. Therefore, studying the deformation behavior of tunnels in weak rock mass is significant in resolving the engineering problems.

During tunnel excavations, the deformation of the rock mass caused by the unloading of itself will vary with time. In the past few decades, the radial shape of the displacements around the tunnel face has been estimated. In the mid-1970s, numerical methods were used to analyze the displacement around the tunnel face, thereby obtaining valuable

* Corresponding authors.
E-mail addresses: lyb@chd.edu.cn (Y. Luo), chenjx1969@163.com (J. Chen).

http://dx.doi.org/10.1016/j.tust.2017.10.003
Received 11 October 2016; Received in revised form 8 September 2017
Available online 20 October 2017

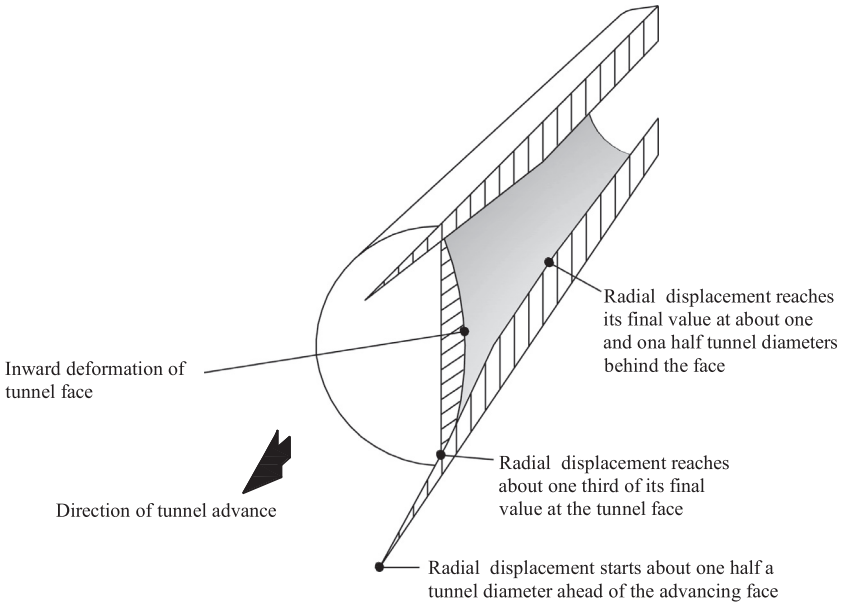

Fig. 1. The deformation pattern in the rock mass that surrounds an advancing tunnel.

information on the stability of the tunnel (Ranken and Ghaboussi, 1975; Hocking, 1976). From the 1980s, monitoring measurement has been extensively used to assess the response of the rock mass based on the field measurements of the rock mass deformation using special instruments (e.g., tap extensometer and precision level) (Sakurai and Takeuchi, 1983; Gioda and Sakurai, 2010). The measured results can reflect the behavior of the rock mass and supporting structures, as well as evaluate the stability of the tunnel structures (Lai et al., 2016b; Luo et al., 2016, 2017a, 2017b; Schubert et al., 2002). However, the measured displacement of the rock mass is only a part of the complete deformation.

Complete deformation includes those before, during, and after the tunnel excavation. Hoek (1998) used a three-dimensional finite element method (FEM) to analyze the rock mass deformation that surrounds a circular tunnel advancing through a weak rock mass, thereby showing a deformation pattern in the rock mass that surrounds an advancing tunnel (Fig. 1). Carranza-Torres and Fairhurst (2000) established a longitudinal deformation profile (LDP) to analyze and graph the radial displacements along the axis of the tunnel in sections located ahead and behind the tunnel face (Fig. 2). With respect to distance from the tunnel face, LDP includes three components: (1) Y_1, pre-deformation, (2) Y_2, loss displacement, which cannot be measured before the installation of the monitoring instrument, and (3) Y_3, measured displacement.

LDP for a tunnel is important to determine the appropriate timing

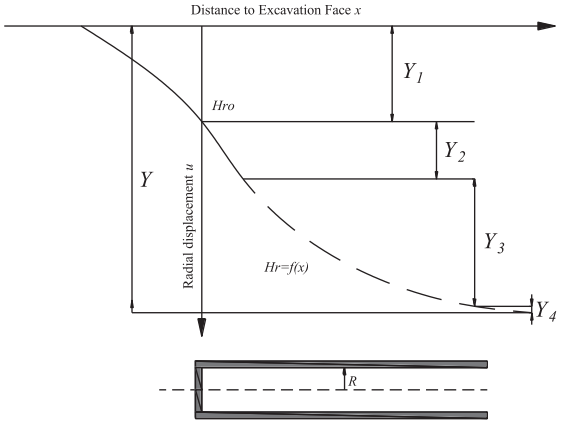

Fig. 2. The radial displacements along the axis of the tunnel in sections located ahead and behind the tunnel face.

for the installation of support or to optimize the installation of support with specific displacement capacity (Song et al., 2016). Two methods are used to obtain LDP, namely, field measurement and numerical simulation. Dr. Zhao (2010) introduced the rock mass deformation of Gui Pu tunnel in Japan, and the space distribution characteristics of a tunnel crown settlement was tested by setting an approximately 50 m-horizontal monitoring tube above the crown of the tunnel surface along the longitudinal of the tunnel. Moreover, Chinese scholars (Zhao, 2010; Li et al., 2014) obtained the data of ground settlement in shallow tunnels. The field measurement data indicated that the pre-deformation Y_1 was located in the crown and ground of the tunnels. Many attempts were used to measure LDP in the field, however, the results were incomplete because the monitoring measurement is difficult to obtain, particularly in deeply buried tunnels. By contrast, numerical simulation is extensively used with the development of computer technology. Numerical simulation includes finite element method (FEM), finite difference method and discrete element method (Jiao et al., 2005). However, the material parameters of the ground are difficult to determine in a numerical simulation. The material properties are affected by the inhomogeneous nature of the soil mass or rock mass, and the influence of complicated geological factors (Liang et al., 2003).

The back analysis method was first introduced to obtain the actual material parameters during tunnel construction in 1980s (Cividini et al., 1981). Back analysis is an effective indirect technique that uses displacements (Sakurai and Takeuchi, 1983; Gioda and Sakurai, 2010), strains (Sakurai et al., 2010), stresses (Kaiser et al., 1990), or acoustic emission information (Cai et al., 2007) to obtain the material parameters. Moreover, back analysis has been extensively used in underground engineering and has become increasingly popular in solving engineering problems (Yeh and Yoon, 1981; Cividini et al., 1983; Okabe et al., 1998; Li et al., 2001; Lee et al., 2006; Feng et al., 2006; Vardakos et al., 2007; Hudson and Feng, 2007; Guan et al., 2009). Levenber–Marquardt, Gauss–Newton, Bayesian, Powell, Rosenbork, and genetic algorithms have been proposed to obtain the optimal values of the parameters from the measured displacements (Deng and Lee, 2001; Huang et al., 2009; Lai et al., 2016a; Ren et al., 2005; Miranda et al., 2011; Yang et al., 2010; Yu et al., 2007). However, problems remain unresolved. For example, searching for the estimated parameter values is difficult in a large and considerably multimodal space (Khamesi et al., 2015).

This study based on a weak rock mass tunnel in the Mingyazi tunnel in Shaanxi Province of China to measure the tunnel displacement in

site, including the crown settlement (vertical displacement) and horizontal displacement. The LDP of this tunnel was analyzed by numerical simulation using the FLAC (a simulation software developed by American ITASCA Company). Back analysis method was used to obtain the rock mass parameters utilizing the measured data in a weak rock mass tunnel. The summed squared errors between the calculated displacements and their corresponding observed values were used for the golden section method (Zhang et al., 2011). The golden section method was used to determine the parameters λ and E only by utilizing the measured crown settlement (Cai et al., 2007; Deng and Lee, 2001; Li et al., 2001; Sakurai and Takeuchi, 1983; Yu et al., 2007). In this paper, the study is improved given that the crown settlement and horizontal displacement were used together to obtain the parameters in a weak rock mass tunnel. Thereafter, the LDP character was studied in a weak rock mass tunnel with different construction schemes to guide the construction and verify the benefit of the optimize construction scheme.

2. Displacement back analysis based on field deformation monitoring

2.1. Engineering example

2.1.1. Overview of the Mingyazi tunnel

The entrance and exit of the Mingyazi tunnel are located in Shuimogou and Shiligou, respectively, in Shiquan County, Shaanxi Province of China, as well as control engineering of the highway construction from Shiyan to Tianshui. The Mingyazi tunnel is a highway tunnel of four-lane in two tunnel bores, and the spacing between the two bores is 40 m. The stake numbers of the entrance and exit at left line are ZK209 + 306 and ZK214 + 255, respectively, and those of the right line are YK209 + 325 and YK214 + 310. The left and right lines are 4949 m and 4985 m in length, respectively, both are extra-long tunnels. Moreover, the maximum buried depth of both tunnels is 320 m.

The geological and hydrogeological conditions of this tunnel are very complex. The design of them was revised frequently by the exposed tunnel face condition. We can see that the exposed tunnel surfaces are soft ground, and much folding and faulting has occurred in ground, as shown in Fig. 3. As a result of diverse geological, sampling, the physical and mechanical indices of engineering soft ground showed that the rock is siliceous limestone of color from dark yellow to light black. There are abundant joints and quartz dike in the tunnel rock mass. The outcrop of rock are dark calcareous slate and shale of interbed with siliceous limestone. This rock will be soften easily by water due to the low unconfined compressive strength of them at saturated situation, especially the calcareous shale is easily creeping and slipping at surface which become smooth after encounter water. The rock mass is weak and lead to inevitable lager deformation in tunnelling.

The design of Mingyazi tunnel accorded to the principle of New Austrian Tunnelling Method (NATM) (Golser, 1976) which has been broadly applied due to its simple, adaptive, cost effective and technical feasibility (e.g., Kolymbas, 2005; Fang et al., 2012; Zhang et al., 2013; Li et al., 2016). The tunnel support comprises primary support, layer of watertight and secondary lining as shown in Fig. 4. The primary support includes forepoling of seamless grouted steel tube, steal frame, shotcrete, feet-lock pipe and mesh reinforcement, the layer of watertight includes drainage facilities and waterproof measures, the secondary lining is segmental cast reinforced concrete.

The construction of Mingyazi tunnel used the NATM. In order to promote the tunnel face stability and to reduce rock mass displacement, the tunnel face is partitioned either horizontally or vertically to several temporary drifts, which is called the sequential excavation method (SEM) (Sharifzadeha et al., 2013). In Mingyazi tunnel the face was partitioned into three temporary drifts, like upper bench, middle bench and lower bench, which advanced parallel as shown in Fig. 5. Lengths of the upper bench, the middle bench and lower bench were 3 m, 9 m and 27 m, respectively. Length of invert construction was 3–5 m. The advance lengths for every step excavation were 1.5 m at upper bench, 4.5 m at middle bench and lower bench, which are strictly restricted to the distance between two steel frames along the tunnel longitudinal axis.

During tunnelling the design of construction scheme was dynamically optimized according to the situation of rock mass and the ability of worker and facilities. There are two steps for the optimizing, first is to change the lengths of bench that the upper bench, the middle bench and lower bench were 3 m, 6 m and 15 m respectively, second is to change the geometry of primary support that the form of sidewall from straight to curving and make sure the side wall smooth link to the invert which would be added. The final optimized scheme is shown in Fig. 6.

2.1.2. Monitoring scheme

In order to investigate the deformation characteristics of the Mingyazi tunnel with soft rock mass, 9 sections at the similar stratum were selected as testing and monitoring sections. There are 3 sections of YK214 + 047, YK214 + 020 and YK214 + 011 constructed follow the original design scheme and the rest of 6 sections constructed with the optimized scheme. This 6 sections were separated into two parts due to the optimized scheme have two steps, There are 3 sections of YK214 + 005, YK213 + 996 and YK213 + 986 just change the length of bench, and 3 sections of YK213 + 902, YK213 + 897 and YK213 + 880 not only change the length of bench, but also change the geometry of primary support. The stake numbers of those sections and the construction scheme at each section are shown in Table 1.

According to the tunnel situation, the monitoring scheme of field test has been made. As for the traditional measuring method such as level gauge and convergence gauge have obvious shortcomings of untimely reading of the initial value, because of the influence of construction and process, which results in smaller measured value than actual. Therefore, the crown settlement and horizontal displacement were measured by using total station and remote distance measurement (RDM), which can reduce the error and improve accuracy efficiently (Luo et al., 2016). The arrangement of monitoring points in each section is shown in Fig. 7. The test contents, instrument, and frequency are shown in Table 2.

Fig. 3. Site engineering geological condition.

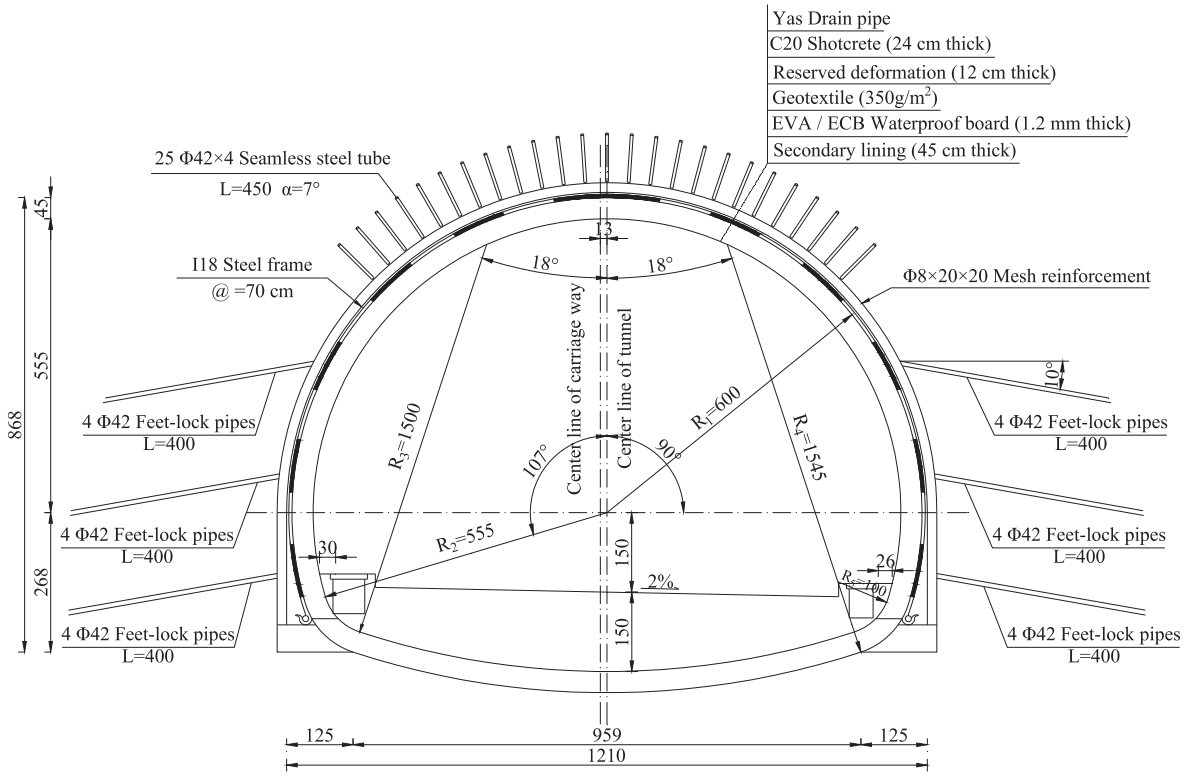

Fig. 4. Support structure of tunnel (V grade rock mass). Note: In this figure, all units are written in cm, except the units of feet-lock pipe, mesh reinforcement and forepoling bolts are written in mm.

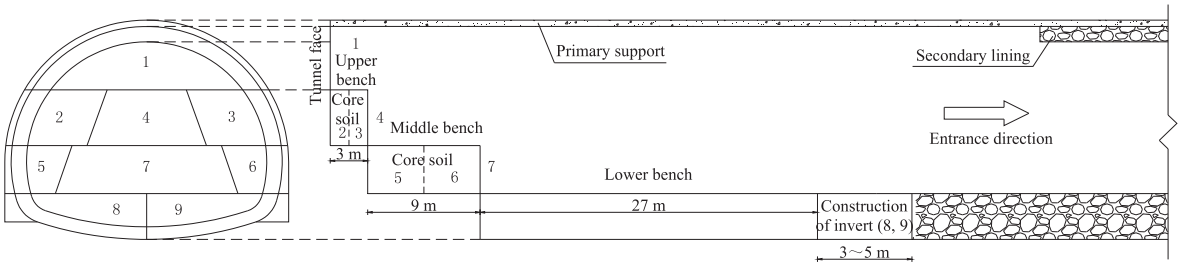

Fig. 5. Construction method of Mingyazi tunnel.

2.1.3. Deformation monitoring data

The monitoring results of each section for horizontal displacement and crown settlement are shown in the Table 3. We can see from Table 3 that the max value of the first three sections is 299.4 mm, and it of the second three sections is 180 mm, and it of the last three sections is 104 mm. This results illustrate that the controlling the tunnel deformation by using the optimized scheme is better than using the original scheme. We can easily get from Table 3 that the crown settlement of left side and right side are different due to the different rock mass at left and right side. However, the simulated model is always a symmetrical structure, i.e., the displacement of left and right side is same. So, in order to balance the difference between simulation and real project, we should choose a section of which the left and right side settlement are the same or virtually the same. The left and right side settlement of YK 214 + 011 section, includes not only the left arch and right arch, but also the left side wall and right side wall, are more close to the same than other sections. The YK214 + 011 section was selected as the typical section to analyze the deformation change with time, as shown in Figs. 8 and 9.

The Fig. 8 shows that the settlement values of every monitoring

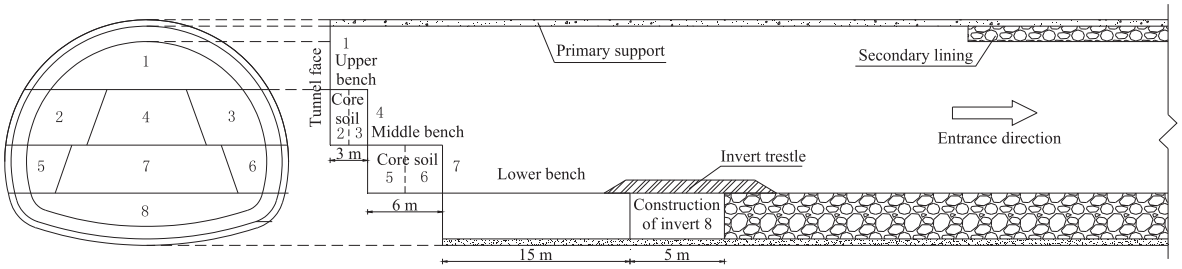

Fig. 6. Optimized construction scheme of Mingyazi tunnel.

Table 1
Construction scheme at each monitoring section.

Sections	Form of side wall	Lengths of bench	Invert	Excavation method of invert
YK214 + 047 YK214 + 020 YK214 + 011	Straight	Upper bench is 3 m Middle bench is 9 m Lower bench is 27 m	No	Left and right invert alternates with each other
YK214 + 005 YK213 + 996 YK213 + 986 YK213 + 902 YK213 + 897 YK213 + 880	Curving	Upper bench is 3 m Middle bench is 6 m Lower bench is15 m	Have	Full size excavated one time utilizing trestle

Table 2
Monitoring scheme of Mingyazi tunnel.

Measurement contents	Instrument	Measurement frequency	
		Time after construction	Frequency
Horizontal displacement	Total station	1–15 Days	Once or twice a day
		16 Days–1 Month	Once a day
		A month later	Once or twice a week
Crown settlement	Total station	1–15 Days	Once or twice a day
		16 Days–1 Month	Once a day
		A month later	Once or twice a week

points are basically stable before the construction of invert. Besides, the lengths of middle and lower bench are too long to achieve the closure of the primary support structure early, which is unfavorable to the stability of tunnel structure. The crown settlement final value is 97 mm, the left and right arch settlement value are larger than the crown. The maximum settlement value appears at the left arch, it reaches 138.7 mm.

The Fig. 9 shows that when the middle bench was excavated, the horizontal displacement increased sharply until the invert was constructed. The horizontal displacement value at the maximum excavation line is larger than that at the upper bench, and the final value at the maximum excavation line is 227.6 mm.

2.2. Back analysis of displacement based on numerical simulation

2.2.1. Establishment of the geometric model

Practice indicates that the model parameters in tunnel displacement back analysis is hardly fully to match the rock mass, they just should reflect the main mechanical characteristics of the rock mass. Yin and Zhu (2004) explained that the elastoplastic model is better than elastic model for simulating the case of soil, and the Mohr-Coulomb criterion is better than Drucker-Prager Criterion. The elastoplastic mechanical parameters of the rock mass can be back inferred from the measured values of the crown settlement and horizontal displacement. The elastic and plastic medium models can comprehensively reflect the main deformation characteristics of the tunnel rock mass. Therefore, this paper assumes that the rock mass is a uniformly continuous elastoplastic media, and the rock mass follows the Mohr-Coulomb criterion. The mesh reinforcement is considered a safety reserve in the calculation, therefore, it is not considered. Besides, it is assumed that the feet-lock pipe and support structure are uniformly continuous and isotropic elastic materials. A few parameters in the model were obtained by tests and field investigation, like cohesion C, Bulk density γ, internal friction angle φ and Poisson's ratio μ. Table 4 provides the model parameters of rock mass, primary support and feet-lock pipe in process of simulation.

In this paper, the YK214 + 011 section of Mingyazi tunnel was selected as the prototype for the numerical simulation. The buried depth of the YK214 + 011 section is 90 m, which belongs to the deep buried section. The tunnel excavation span is 12.38 m. Moreover, the tunnel excavation method was simulated as the original design scheme. Current experience indicate that the rock mass which is 3–5 times the tunnel diameter tunnel away from the hole has limited influence on the tunnel. Restrictions brought about by computational conditions entail that the number of units should be minimized, therefore, the lengths of the upper, lower, left, and right boundaries were all defined as approximately 3 times the excavation span. Accordingly, the length, width, and height of the model are 60, 100, and 100 m, respectively. The tectonic stress field is difficult to simulate due to its complexity and hardly be tested in situ, so there is only a self-weight stress field of the rock mass in the initial state in this paper. A vertical displacement

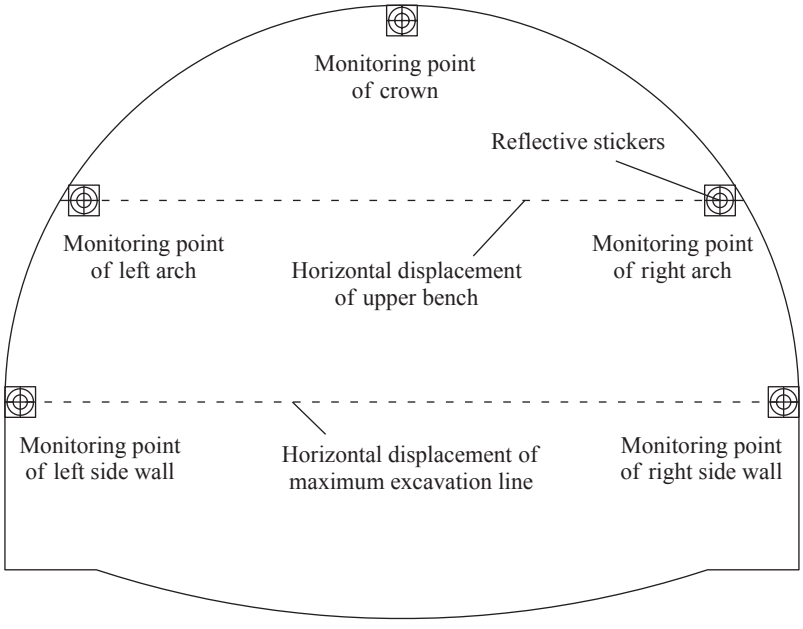

Fig. 7. Arrangement of monitoring points.

Table 3
Monitoring results of each section for deformation.

Sections	Horizontal displacement value		Crown settlement value				
	Upper bench	Maximum excavation line	Crown	Left arch	Right arch	Left side wall	Right side wall
YK214 + 047	107.0	299.4	59.4	48.2	214.8	50.6	264.2
YK214 + 020	46.8	75.0	60.4	59.6	83.2	41.8	66.8
YK214 + 011	107.4	227.6	97.0	139.6	122.0	98.4	94.0
YK214 + 005	–	91.4	55.4	104.0	69.6	71.4	180.0
YK213 + 996	130.0	151.6	101.6	–	–	90.2	–
YK213 + 986	73.4	129.2	78.8	119.2	62.0	73.0	134.2
YK213 + 902	66.1	76.2	80.5	20.0	44.3	71.6	81.8
YK213 + 897	60.1	71.2	63.2	59.7	62.8	58.2	104.0
YK213 + 880	58.2	74.0	69.0	29.0	42.6	35.6	76.4

constraint is applied at the bottom boundary of the model, and the horizontal displacement constraint is applied at the left, right, front and back boundaries of the model. The feet-lock pipes are set as beam elements and the others (primary support, secondary lining and rock mass) are set as brick elements. The model consists of 192003 nodes and 182400 units as shown in Fig. 10.

2.2.2. Selection of the calculation parameters

In the back analysis process of the rock mass, determining the stability of the rock mass is difficult because of discontinuity, heterogeneity of the rock mass, limited location of the mechanical monitoring points, limited field stress test range, and substantially large discreteness of the measured value. Compared with the stress and strain measurements of the tunnel, the rock mass deformation has larger measurement range and is easier to be measured, thus, rock mass deformation can intuitively and accurately build a relationship with the stability of the rock mass. So, the rock mass parameters were back analyzed by the measured deformation.

The main parameters of the elastoplastic models of the rock mass are the elastic modulus E, lateral pressure coefficient λ, Poisson's ratio μ, internal friction angle φ, and cohesion c. Among them, the Poisson's ratio μ, internal friction angle φ, and cohesion c can be obtained through indoor experiments, thus, these parameters are the known parameters in the back analysis of the tunnel. By contrast, obtaining the accurate elastic modulus E is considerably difficult because the elastic modulus of the rock obtained from test is different from the actual elastic modulus. If we use the tested elastic modulus to analyze and calculate the rock engineering, the results obtained are often different from the actual engineering practice. In this paper, the elastic modulus E is used as one of the back-stepping parameters in the displacement back analysis.

Numerous engineering practices and theoretical studies show that the initial stress of the rock mass must be considered in designing and constructing tunnels because it substantially influences the tunnel excavation method and support parameters. The lateral pressure coefficient λ is theoretically determined by the formula (1).

$$\lambda = \mu/(1-\mu) \tag{1}$$

where μ is the Poisson's ratio of the rock mass with a value between 0 and 0.5, whereas the Poisson's ratio of the majority of the rock mass is between 0.15 and 0.35. The maximum lateral pressure coefficient calculated by formula (1) is 1, although a value above 1 is also common in tunnel engineering practice. Therefore, the lateral pressure coefficient cannot be determined based on the formula (1) and should be determined according to the back analysis of the field measurements or statistical data (Azevedo et al., 2002). In this paper, the lateral pressure coefficient λ is used as one of the back-stepping parameters in the displacement back analysis.

Table 4 lists the physical and mechanical parameters of the rock mass based on the *Highway Tunnel Design Code* (D70 JTG-2004) in China, and the site geological survey data. In this paper, the lateral pressure coefficient λ and elastic modulus E are used as the back-stepping parameters in the displacement back analysis. The value range of λ and E is provided based on the specifications and field conditions.

2.3. Displacement back analysis method

The golden section method is an effective and simple algorithm, and it is used to derive the minimum of the function. In the process of determining the minimum function value within the independent and variable value range, the golden section method can be used to systematically narrow the range to obtain the minimum value of the function.

If the minimum value of the function $f(x)$ in the range of (a, b) exists, assuming that a < b, then c and d are two segmented points in (a, b) that meet the following formula (2).

$$\begin{cases} c = (1-\alpha)\cdot a + \alpha\cdot b \\ d = \alpha\cdot a + (1-\alpha)\cdot b \end{cases} \tag{2}$$

where α is the golden section coefficient ($\alpha = 0.618$). The diagram of the golden section method is shown in Fig. 11.

The values of c and d can be obtained through the golden section method, hence, c > d because that a < b. Taking the value of c as a, d

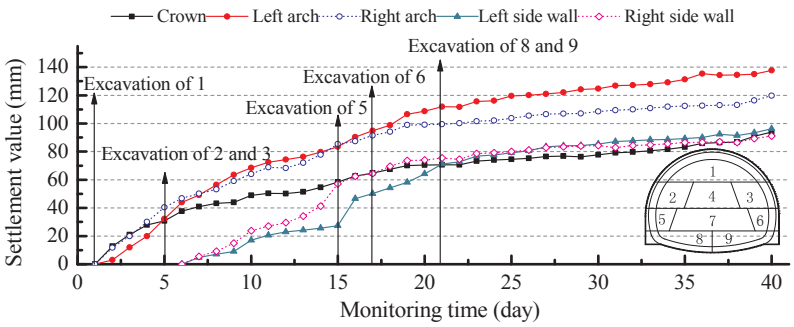

Fig. 8. Crown settlement temporal curve of YK214 + 011.

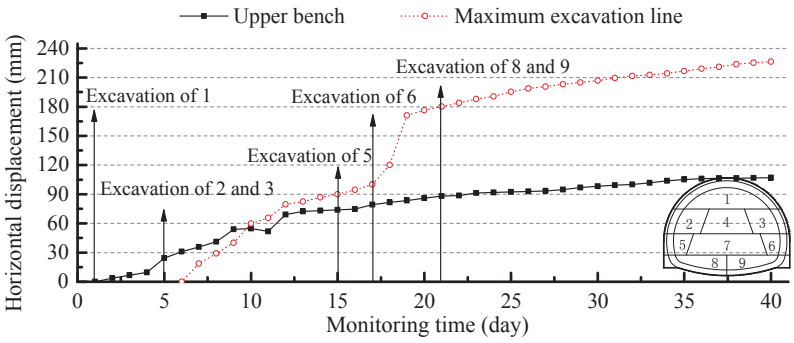

Fig. 9. Horizontal displacement temporal curve of YK214 + 011.

as b, then put c and d in $f(x)$ to obtain $f(c)$ and $f(d)$, and comparing the values.

(1) If $f(c) > f(d)$, then (a, c) will be considered a new value interval (a_1, b_1) $(a_1 = a, b_1 = c)$ to continue the segmented calculation.
(2) If $f(c) < f(d)$, then (d, b) will be considered a new value interval (a_1, b_1) $(a_1 = d, b_1 = b)$ to continue the segmented calculation.

In continuing the calculation, the value interval will be gradually narrowed until it approximates the minimum value that satisfies the accuracy requirement. The coefficient $\alpha = 0.618$, hence, the segmented point c or d obtained in the last round of calculation is still among the segmented points in the new value interval. Each calculation round can effectively narrow the value interval, thereby effectively reducing the calculation times.

When two independent variables are present, the golden section method is still applicable. In this situation, one of the independent variables is replaced by an appropriate estimated value and the other one is calculated using the fore mentioned method. This way, the process can be simplified to involve only one independent variable. After the extreme value is obtained, the value will be taken in the function $f(x)$ as a known value, and the segmented calculation of the other independent variable is performed until the optimal solution is obtained. This method is also known as coordinate alternation (Dong, 2009).

2.4. Displacement back analysis based on numerical simulation

Assuming that the tunnel deformation equation in the numerical simulation is:

$$g(x) = g(E,\lambda) \tag{3}$$

The monitoring value of the tunnel deformation is D and the objective function is:

$$f(x) = |g(E,\lambda) - D| \tag{4}$$

The values of E and λ, which can make the function (3) yield a minimum value, are the optimum solution that needs to be solved. The function (4) can be calculated by using different parameters into the three dimension FLAC model and the value of D can be obtained through field monitoring data. This study uses the monitoring data of the YK214 + 011 section. Moreover, the crown settlement value is $D_1 = 97.0$ mm and the horizontal displacement value of the maximum excavation line is $D_2 = 227.6$ mm.

Chen (2013) showed that the change of elastic modulus has immense influence on the crown settlement but has limited influence on the horizontal displacement. Therefore, the elastic modulus E was back calculated first based on the crown settlement data, and then the lateral pressure coefficient λ was back calculated based on the horizontal displacement of the maximum excavation line. The crown settlement and horizontal displacement data were measured from the YK214 + 011 section in the Mingyazi tunnel. The back calculating uses the monitoring data and the numerical simulation data. The simulation process of tunnel excavation is shown in Fig. 12.

2.4.1. Back analysis of the elastic modulus E

The value of the elastic modulus E is (0.2, 1) and the value of the lateral pressure coefficient λ is (0.3, 1.5). One of the parameters should be fixed based on the principle of the multi-parameter golden section method. In this paper, the lateral pressure coefficient λ is initially fixed (i.e., λ = 1.0), then carried over to the segmented calculation of the elastic modulus E. Table 5 shows the calculation results.

Table 5 shows that when $E = 0.2992$ GPa, the objective function value is only 0.2 mm and the relative error is only 0.02%. Therefore, the results meet the requirements of the back analysis.

2.4.2. Back analysis of the lateral pressure coefficient λ

The elastic modulus has been determined (i.e., $E = 0.2992$ GPa) based on the back analysis of the elastic modulus E. Thereafter, the segmented calculation of the lateral pressure coefficient λ is performed. Table 6 shows the calculation results.

Table 6 shows that when λ = 1.2576, the objective function value is only 0.4 mm and the absolute error is only 0.2%. Therefore, the results meet the requirements of the back analysis.

2.4.3. Analysis of the back analysis results

To verify the accuracy and reliability of the back-stepping parameters, the elastic modulus E of the rock mass and the lateral pressure coefficient λ, which obtained by using the back analysis, were input into the three dimension FLAC model to calculate the crown settlement and horizontal displacement values on the maximum excavation line. Time-step diagrams of displacement can be obtained by comparing the calculated values with the monitoring data (as shown in Figs. 13–15).

The final calculated crown settlement value is 114.9 mm, which is

Table 4
Model characteristic parameter list.

Material category	Elastic modulus E (GPa)	Poisson ratio μ	Bulk density γ (kN/m)	Cohesion C (MPa)	Internal friction angle (°)	Lateral pressure coefficient λ
Rock mass	0.2 ~ 1	0.35	24	0.15	24	0.3 ~ 1.5
The primary support (including steel)	26.8	0.16	25			
Anchor bolt	210	0.2	77			

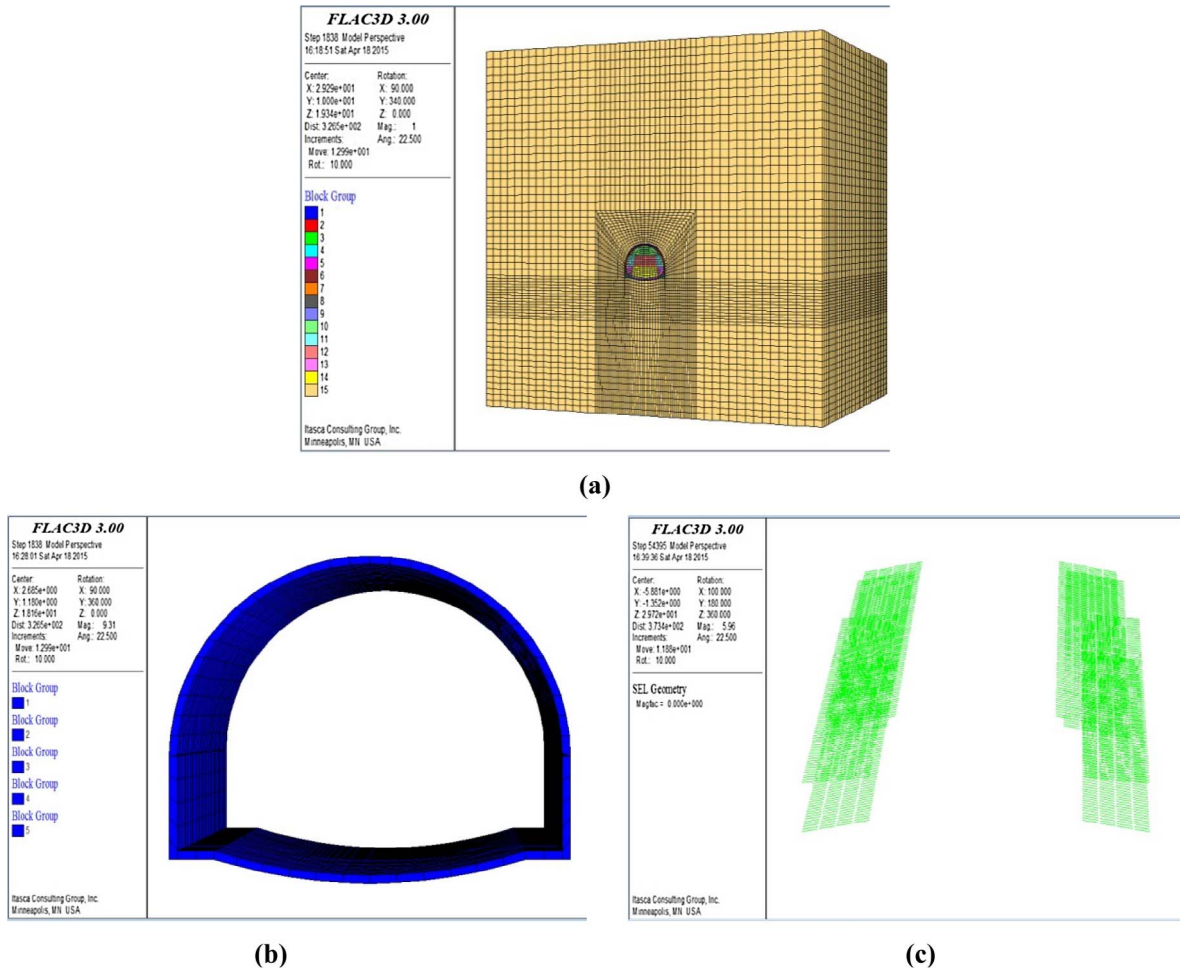

Fig. 10. Geometric model diagram (a) and shotcrete model diagram (b) and feet-lock pipe model diagram (c).

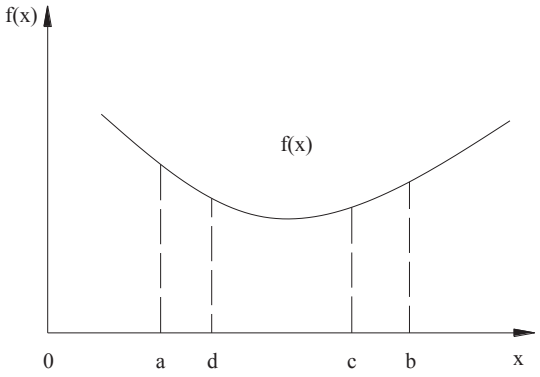

Fig. 11. Sketch of golden section method.

the complete displacement. The calculated displacement before the construction of the initial support is 12.9 mm, as well as it includes the pre-deformation and the loss displacements (as shown in Fig. 13). The calculated crown settlement value can be obtained by subtracting the pre-deformation and the loss displacements from the complete displacement, therefore, the calculated crown settlement value is 114.9–12.9 = 102.0 mm. This value can be compared with the field monitoring data. The measured crown settlement value is 97 mm, and the difference between the calculated and measured values of the crown settlement is 5.0 mm with a relative error of 5.2%. The calculated and measured horizontal displacements are 228.0 mm (as shown in Figs. 14 and 15) and 227.6 mm, respectively. Moreover, the difference between the calculated and measured values of the horizontal displacement is 0.4 mm with a relative error of 0.2%. Overall, the back analysis error is relatively small.

2.5. Analysis of the influence of the rock mass parameters E and λ on tunnel deformation

The elastic modulus E was analyzed by changing the value from 0.6944 GPa to 0.2992 GPa, when maintaining $\lambda = 1.0$. The calculations of the tunnel crown settlement and horizontal displacement on the maximum excavation line are shown in Fig. 16.

Thereafter, the lateral pressure coefficient λ was analyzed by changing the value from 0.7584 to 1.2576, when maintaining $E = 0.2992$ GPa. The calculations of the tunnel crown settlement and displacement on the maximum excavation line are shown in Fig. 17.

The Figs. 16 and 17 show that the λ is positively related to the deformation, while the E is negatively related to the deformation. The greater absolute values of slope for the lines are, the greater effect of relevant parameters for rock mass on the deformation. The absolute value of slope for E-crown settlement line and E-horizontal displacement line are 149.1 and 317.6, respectively (as shown in Fig. 16). The absolute value of slope for λ-crown settlement line and λ-horizontal displacement line are 189.0 and 79.67, respectively (as shown in Fig. 17). Therefore, the elastic modulus of the rock mass has greater influence on tunnel deformation than the lateral pressure coefficient. Moreover, the change of the lateral pressure coefficient λ has a greater influence on crown settlement than that on the horizontal displacement (as for 189 > 79.67).

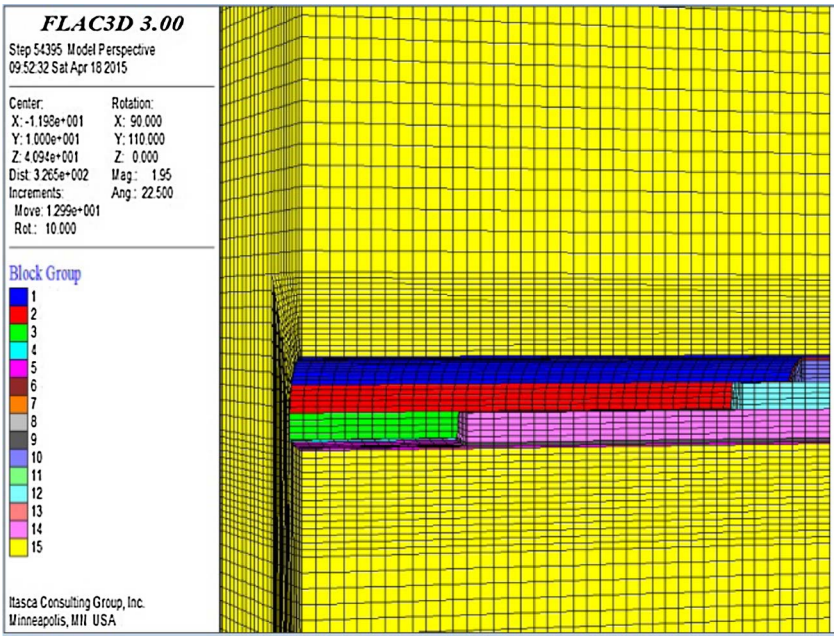

Fig. 12. Tunnel excavation simulation diagram.

Table 5
Back analysis results of elastic modulus.

Elastic modulus (GPa)	Lateral pressure coefficient	Calculated crown settlement (mm)	Measured crown settlement (mm)	Objective function (mm)	Absolute error (%)
0.6944	1.0	41.2	97	55.8	57.5
0.5056	1.0	56.9	97	40.1	41.3
0.3888	1.0	74.2	97	22.8	23.5
0.3168	1.0	91.3	97	5.7	5.9
0.2720	1.0	106.8	97	9.8	10.1
0.3440	1.0	84.0	97	13.0	13.4
0.2992	1.0	96.8	97	0.2	0.02

Table 6
Back analysis result of lateral pressure coefficient.

Lateral pressure coefficient	Elastic modulus (GPa)	Calculated horizontal displacement (mm)	Measured horizontal displacement (mm)	Objective function (mm)	Absolute error (%)
1.0416	0.2992	210.1	227.6	17.5	7.7
0.7584	0.2992	189.6	227.6	38.0	16.7
1.2168	0.2992	224.0	227.6	3.6	1.6
1.3248	0.2992	236.1	227.6	8.5	3.7
1.1496	0.2992	218.0	227.6	9.6	4.2
1.2576	0.2992	228.0	227.6	0.4	0.2

3. Complete displacement analysis based on the back analysis

3.1. Introduction of the two construction schemes

We know that the section of YK214 + 011 used the original construction scheme and the displacement of it was substantially large, therefore, the original construction scheme was optimized thereafter. In order to simplify the simulation we only consider the first step of optimized construction scheme which just change the length of bench. We can call the original construction scheme is the three long-beach construction scheme, and the first step of optimize construction scheme is the three short-beach construction scheme. So in the complete displacement analysis there are two construction schemes, including the three long-beach construction scheme and the three short-beach construction scheme. The parameters of the rock mass obtained through back analysis were input into the numerical model to establish the LDP. From the LDP, the complete displacement situation under two different construction scheme conditions was analyzed.

3.2. Comparative analysis of the crown settlement variation law

The complete displacement situations of the crown settlement under two construction scheme conditions are shown in Figs. 18 and 19. The abscissa in Figs. 18 and 19 is the ratio of L (distances from monitoring points to tunnel face of upper bench) to D (diameter of the tunnel, the value is 10.5 m). The negative value of L/D means the monitoring point is behind the tunnel face, i.e. the excavated section, on the contrary, the positive value of L/D means the monitoring point is in front of the tunnel face, i.e. the unexcavated section. The crown settlement under different construction scheme caused by each process are shown in Figs. 20 and 21.

The variation law of crown settlement under two different construction scheme conditions is similar. The crown settlement tended to stabilize gradually after the invert was constructed. The pre-deformation of crown settlement within one time the tunnel diameter in front of tunnel face is considerably large, while the pre-deformation of crown settlement over that range is small (as shown in Figs. 18 and 19). The rate of pre-deformation under two different construction scheme conditions is nearly the same, which accounted for approximately 18% of the complete displacement. This indicate that decreasing the lengths of the middle and lower benches has limited influence on the value and scope of the pre-deformation at the crown.

Comparing Figs. 18 and 19, it is found that when using the three short-beach construction scheme, the crown settlement value is 98.7 mm, which is 17.8 mm smaller than that under the original construction scheme condition. This results indicate that measures of shorting the lengths of middle and lower bench and closing the invert early and immediately will benefit the tunnel stability.

Comparing Figs. 20 and 21, it is found that except the process of after the construction of invert the rate of every process under two different construction scheme conditions is nearly the same. When using the three short-beach construction scheme, the crown settlement value after the invert constructed accounts for 8.1% of the crown complete displacement, which is 4.3% larger than that under the three long-beach construction scheme condition. The reason is the early

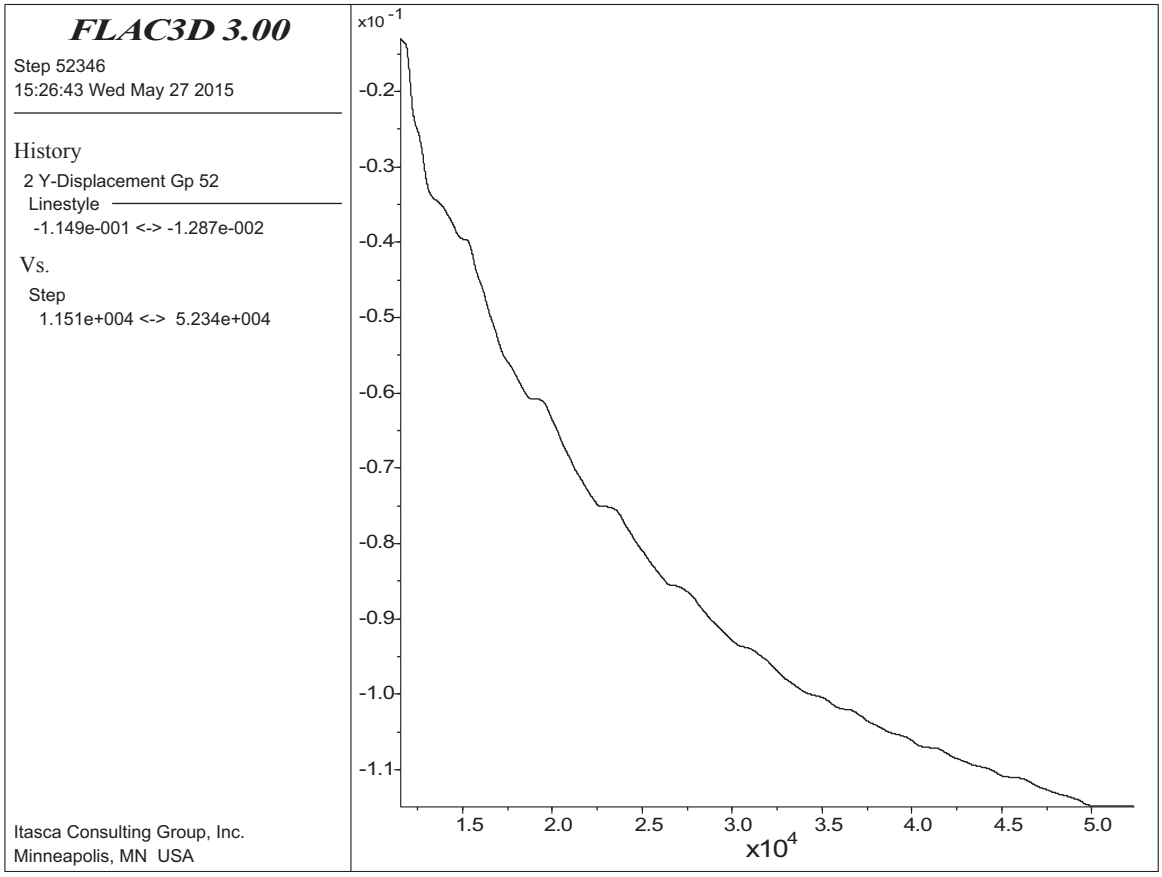

Fig. 13. Time-step diagram of crown settlement.

construction of the invert and the ongoing deformation process of the rock mass.

3.3. Comparative analysis of the horizontal displacement variation law

The complete displacement situations of the horizontal displacement under the two construction scheme conditions are shown in Figs. 22 and 23. The horizontal displacement situations caused by each

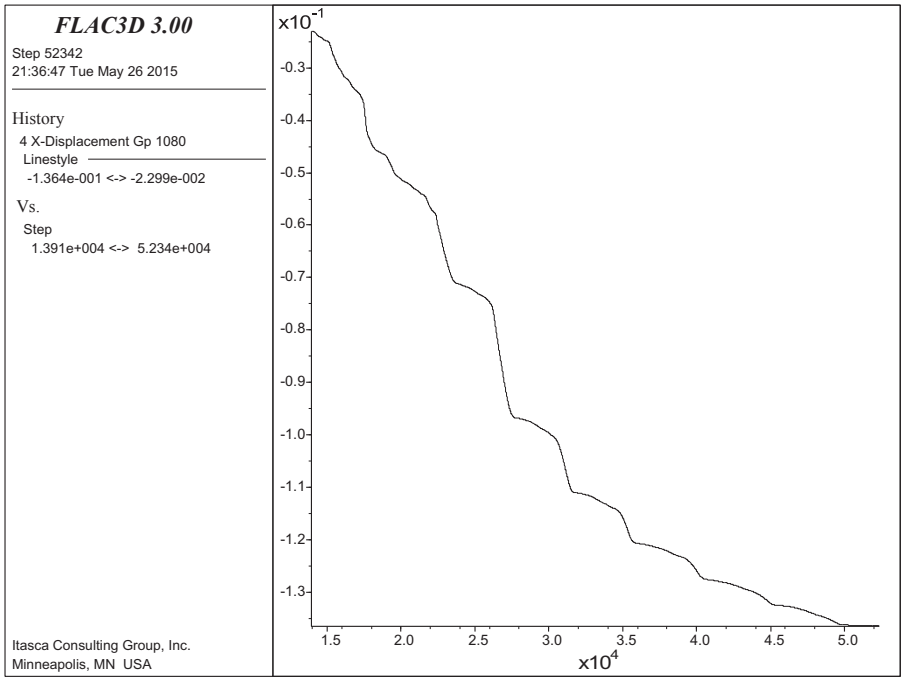

Fig. 14. Time-step diagram of horizontal displacement in left side of tunnel.

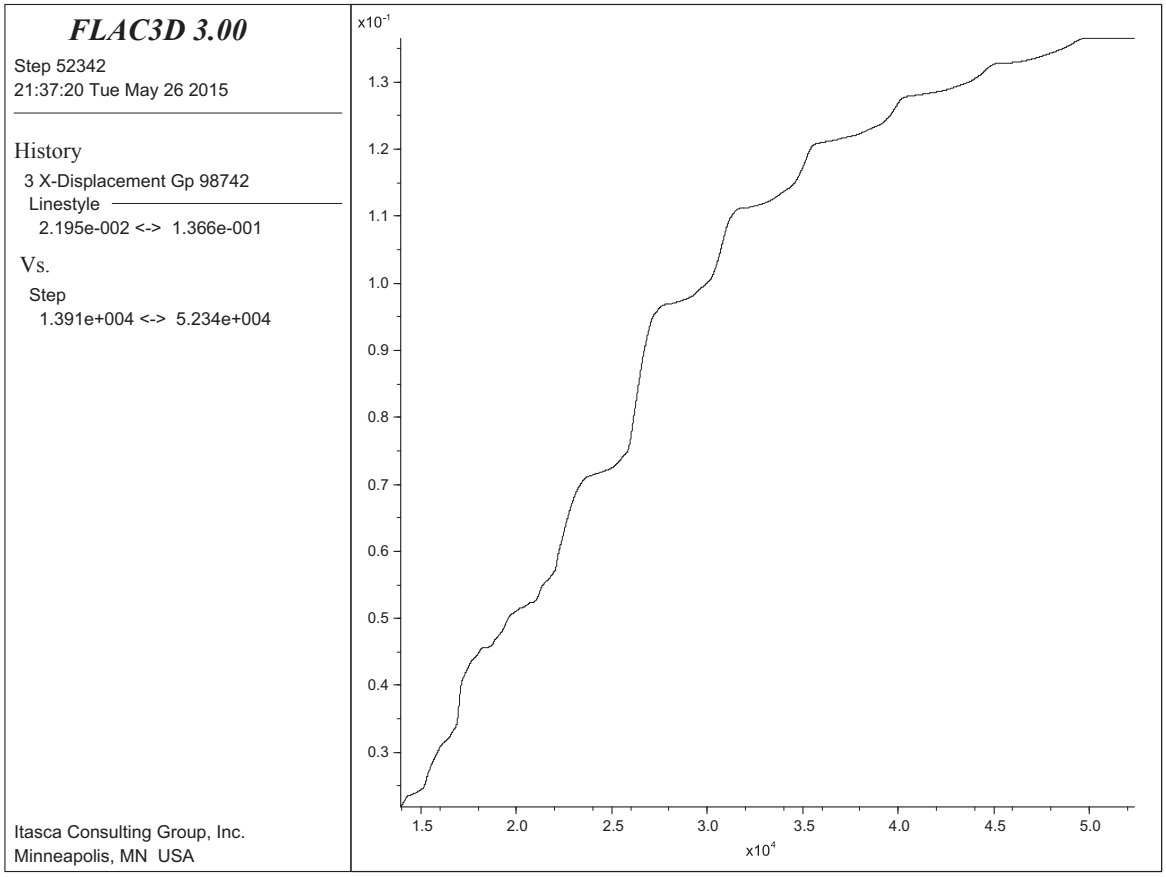

Fig. 15. Time-step diagram of horizontal displacement in right side of tunnel.

process are shown in Figs. 24 and 25.

The variation law of horizontal displacement under two different construction scheme conditions is similar. The horizontal displacement tended to stabilize gradually after the invert was constructed. The pre-deformation of the horizontal displacement within one time the tunnel diameter in front of the tunnel face is large, while the pre-deformation of the horizontal displacement exceed that range is small (as shown in Figs. 22 and 23). The rate of pre-deformation under two different construction scheme conditions is nearly the same, which accounted for approximately 19% of the complete displacement. This indicate that decreasing the lengths of the middle and lower bench has limited influence on the value and scope of the pre-deformation of horizontal displacement.

Comparing Figs. 22 and 23, it is found that when using the three short-beach construction scheme, the horizontal displacement value is 248.2 mm, which is 36.1 mm smaller than that under the original construction scheme condition. This results also indicate the former conclusion that measures of shorting the lengths of middle and lower bench and closing the invert early and immediately will benefit the tunnel stability. The reason is that the lengths of the middle and lower bench have been shortened in the three short-beach construction scheme, thereby enabling the early construction of the invert and the immediate closure of the supporting structure.

Comparing Figs. 24 and 25, it is found that except the process of after the construction of invert the rate of every process under two different construction scheme conditions is nearly the same. When using the three short-beach construction scheme, the horizontal displacement value after the invert was constructed accounts for 7.8% of the horizontal complete displacement, which is 2.9% larger than that under the three long-beach construction scheme condition. The reason

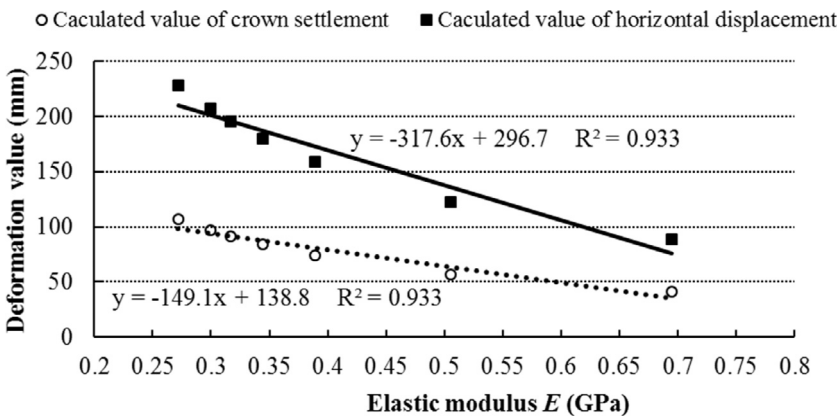

Fig. 16. Calculated value of tunnel deformation change with elastic modulus.

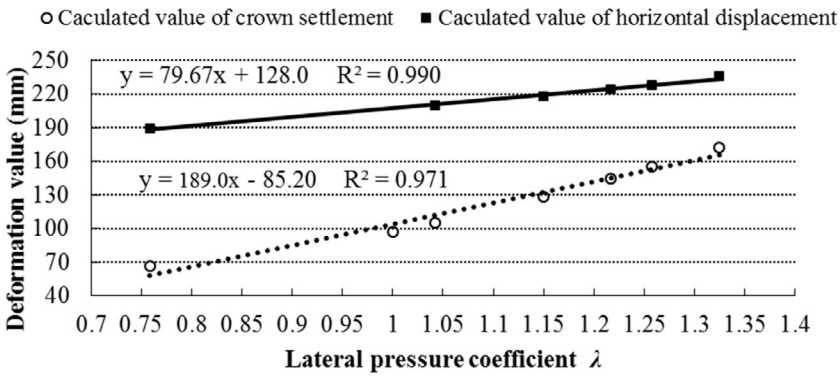

Fig. 17. Calculated value of tunnel deformation change with lateral pressure coefficient.

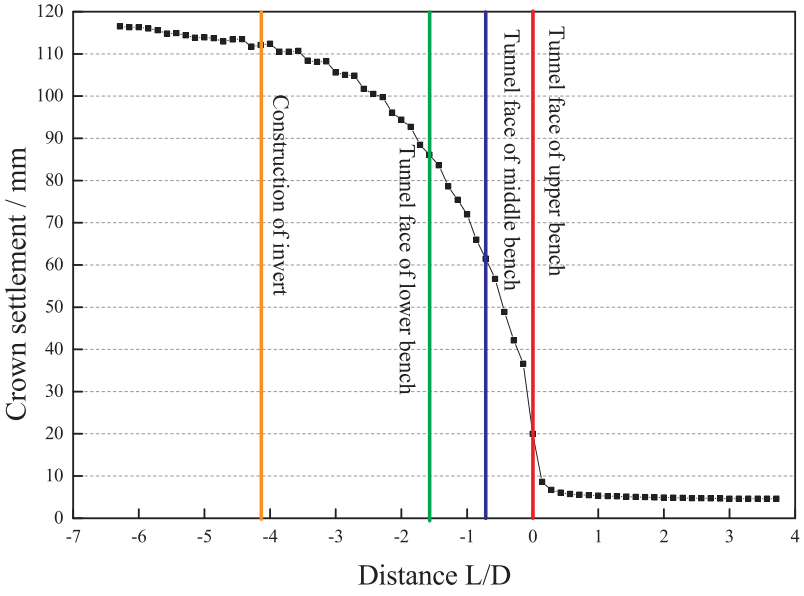

Fig. 18. Crown settlement curve of the original construction scheme.

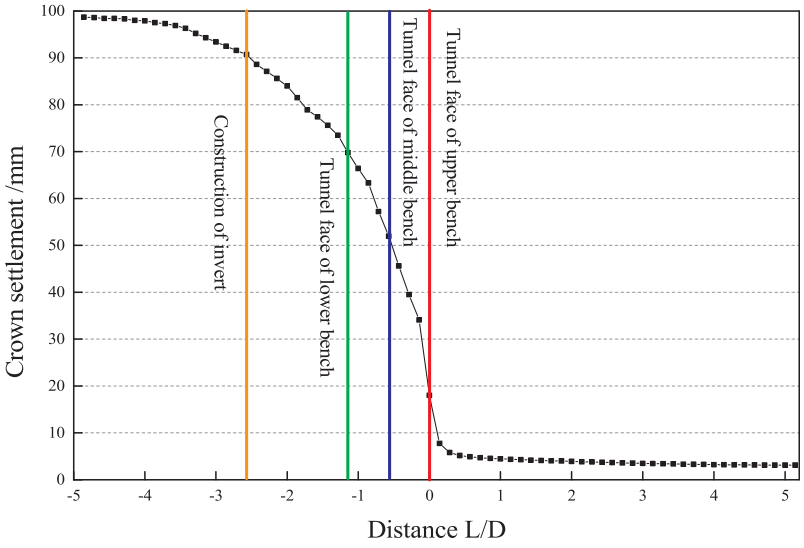

Fig. 19. Crown settlement curve of the optimized construction scheme.

is the early construction of the invert and the ongoing deformation process of the rock mass.

3.4. Comparative analysis of the extrusion deformation variation law

The situations of extrusion deformation on the tunnel face under two construction scheme conditions are shown in Figs. 26 and 27.

The maximum extrusion deformation on the tunnel face under the three long-beach construction scheme was 77.6 mm, whereas the maximum extrusion deformation of tunnel face under the three short-beach construction scheme was 86.7 mm (as shown in Figs. 26 and 27). The extrusion deformation of the optimized scheme is larger than that of the original scheme. The reason is that the lengths of the middle and lower bench have been shortened, thereby resulting in the decreasing of

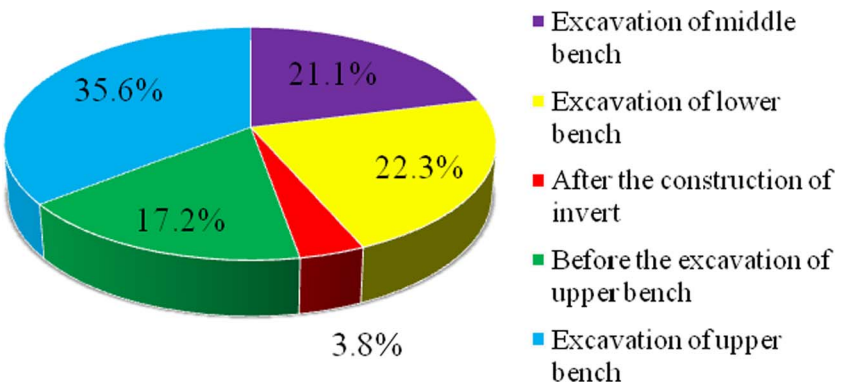

Fig. 20. Crown settlement caused by various processes of the original construction scheme.

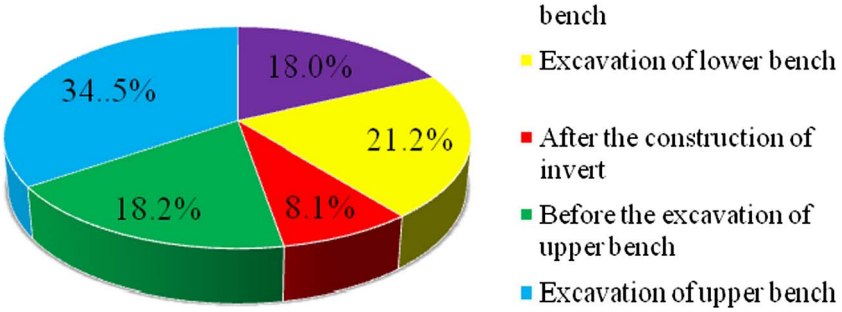

Fig. 21. Crown settlement caused by the processes of the optimized construction scheme.

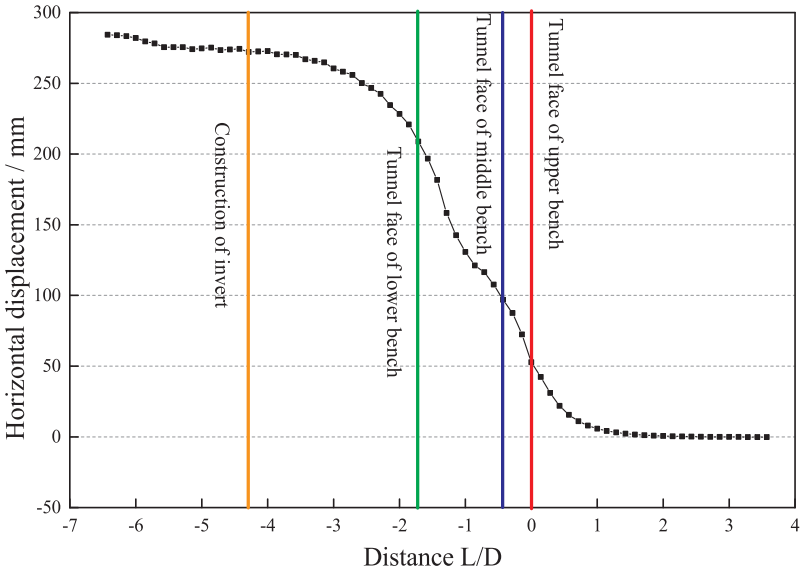

Fig. 22. Horizontal displacement curve of the original construction scheme.

the core soil. Therefore, increasing the area of the core soil is a feasible measure to control the extrusion deformation on the tunnel face.

4. Conclusion

In this study, the tunnel deformation under different construction scheme were tested and monitored in situ, and the LDP was simulated by using the back analysis method in a weak rock mass tunnel. According to the results taken from the in situ monitoring and numerical simulation, the following conclusions can be drawn:

(1) The monitored results illustrate that the controlling the tunnel deformation by using the optimized construction scheme of changing bench length and primary support geometry is better than using the original construction scheme.
(2) The tunnel displacements were affected by the rock mass parameters, namely, the elastic modulus E and the lateral pressure coefficient λ. The change of E has greater influence on the displacement than that of λ, and the change of λ has greater influence on crown settlement than that on the horizontal displacement.
(3) From the simulated LDP the variation law of complete deformation including crown settlement and horizontal displacement under the long-beach and short-beach construction scheme conditions is similar. The tunnel deformation tended to stabilize gradually after the invert was constructed. The pre-deformation of the tunnel deformation within one time the tunnel diameter in front of the tunnel face is large, while the pre-deformation of the tunnel deformation exceed that range is small.

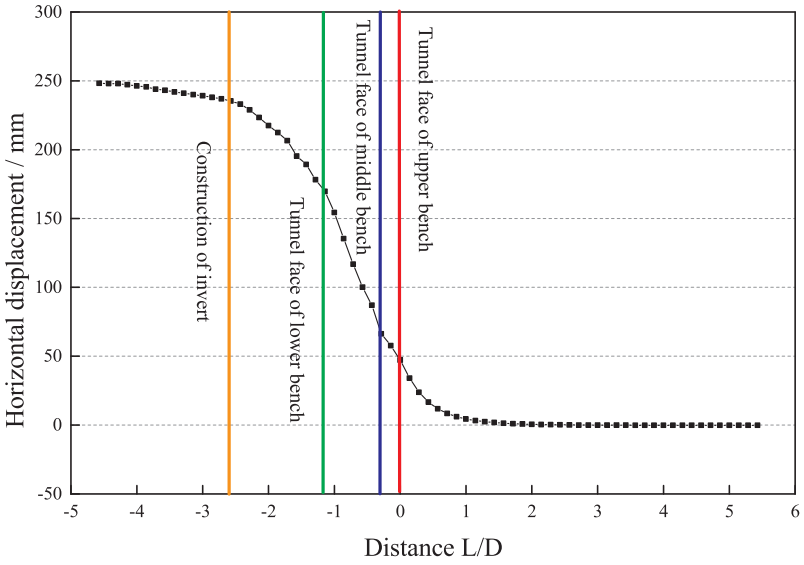

Fig. 23. Horizontal displacement curve of the optimized construction scheme.

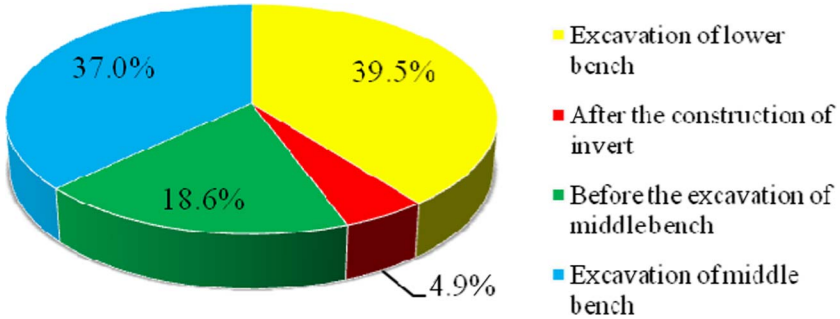

Fig. 24. Horizontal displacement caused by various processes of the original construction scheme.

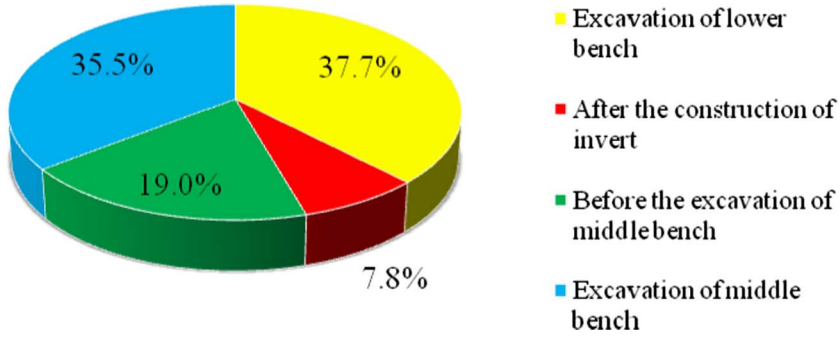

Fig. 25. Horizontal displacement of various processes of the optimized construction scheme.

(4) The rate of pre-deformation under the long-beach and short-beach construction scheme conditions is nearly the same, which accounted for approximately 18% and 19% of the complete displacement for crown settlement and horizontal displacement separately. This indicate that decreasing the lengths of the middle and lower benches has limited influence on the value and scope of the pre-deformation of the tunnel deformation.
(5) When the tunnel construction used the three short-bench scheme (i.e., the upper, middle, and lower benches are 3, 6, and 15 m) in the weak rock mass, the complete displacements of the crown settlement and horizontal displacement are smaller than that under the original construction scheme condition. This results indicate that decreasing the lengths of middle and lower bench and closing the invert early and immediately will benefit the tunnel stability.
(6) The extrusion deformation at the tunnel face of the short-beach construction scheme is larger than that of the three long-beach construction scheme. The reason is that the lengths of the middle and lower bench have been shortened, thereby resulting in the decreasing of the core soil. Therefore, increasing the area of the core soil is a feasible measure to control the extrusion deformation on the tunnel face.

Acknowledgements

The authors would like to acknowledge the financial support provided by the National Natural Science Foundation of China (Grant Nos. 51108034, 51408054 and 51678063), the China Postdoctoral Science Foundation (Grant No.2016 M602738), the Natural Science Basic Research Plan of Shaanxi Province (Grant No.2017 JM5051), the Science and Technology Co-ordinating Innovative Engineering Project of Shaanxi Province (Grant No.2014KTCG01-02), the Key Science and Technology Innovation Team Program of Shaanxi Province (Grant No.2014KCT-29) and the Chang Jiang Scholars Program (Grant No. T2014214).

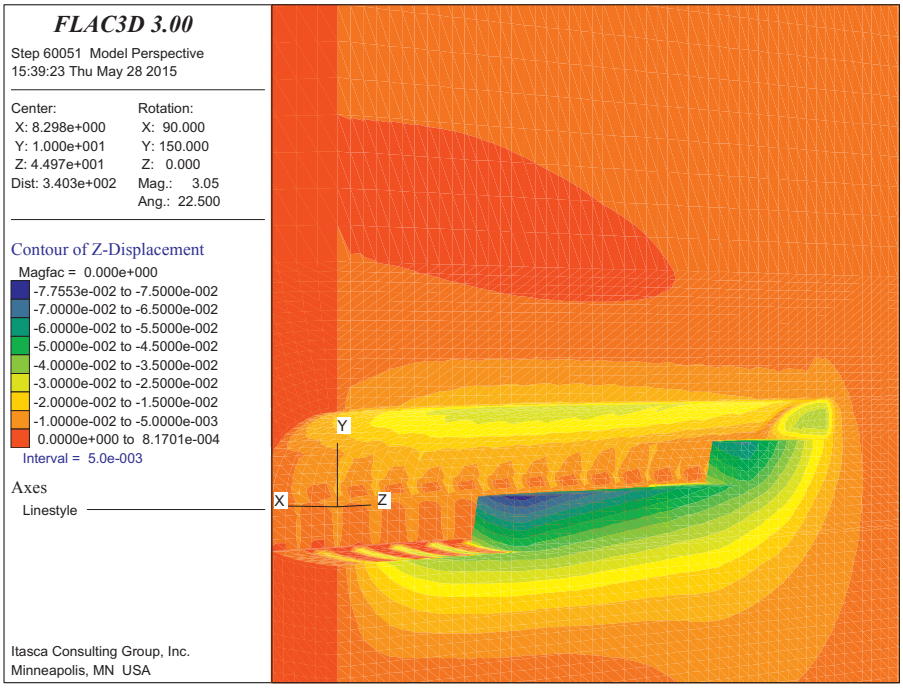

Fig. 26. Tunnel face extrusion deformation nephogram of the original construction scheme.

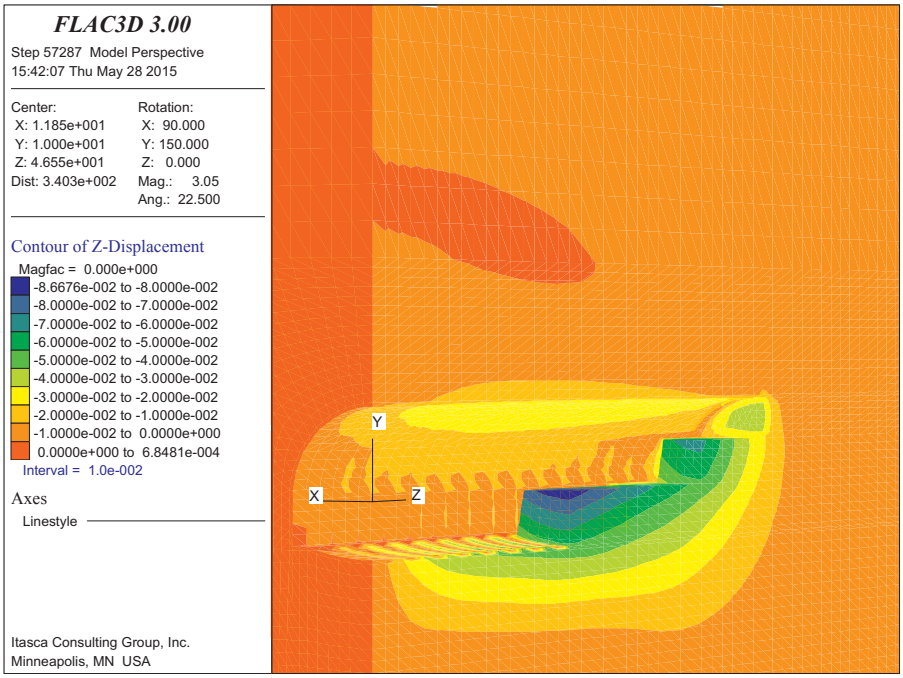

Fig. 27. Tunnel face extrusion deformation nephogram of the optimized construction scheme.

Reference

Azevedo, R.F., Parreira, A.B., Zornberg, J.G., 2002. Numerical analysis of a tunnel in residual soils. J. Geotech. Geoenviron. Eng. 128 (3), 227–236.

Cai, M., Morioka, H., Kaiser, P.K., Tasaka, Y., Kurose, H., Minami, M., Maejima, T., 2007. Back-analysis of rock mass strength parameters using AE monitoring data. Int. J. Rock Mech. Mining Sci. 44 (4), 538–549.

Carranza-Torres, C., Fairhurst, C., 2000. Application of the convergence-confinement method of tunnel design to rock masses that satisfy the Hoek-Brown failure criterion. Tunn. Undergr. Space Technol. 15 (2), 187–213.

Chen, K.J., 2013. The research on tunnel monitoring measurement and data back analysis. Dissertation. Beijing: Beijing University of Technology (in Chinese).

Cividini, A., Maier, G., Nappi, A., 1983. Parameter estimation of a static geotechnical model using a Bayes' approach. Int. J. Rock Mech. Min. Sci. & Geo. Abstr. 20 (5), 215–226.

Cividini, A., Jurina, L., Gioda, G., 1981. Some aspects of characterization problems in geomechanics. Int. J. Rock Mech. Mining Sci. 18 (6), 487–503.

Deng, J.H., Lee, C.F., 2001. Displacement back analysis for a steep slope at the three gorges project site. Int. J. Rock Mech. Mining Sci. 38 (2001), 259–268.

Dong, C.L., 2009. Inversion analysis of tunnel rock parameter based on monitoring and numerical simulation. Dissertation. Wuhan: Wuhan University of Technology (in Chinese).

Fang, Q., Zhang, D.L., Wong, L.N.Y., 2012. Shallow tunnelling method (STM) for subway station construction in soft ground. Tunn. Undergr. Space Technol. 29, 10–30.

Feng, X.T., Chen, B.R., Yang, C.X., Zhou, H., Ding, X.L., 2006. Identification of visco-elastic models for rocks using genetic programming coupled with the modified particle swarm optimization algorithm. Int. J. Rock Mech. Mining Sci. 43 (5), 789–801.

Gioda, G., Sakurai, S., 2010. Back analysis procedures for the interpretation of field measurements in geomechanics. Int. J. Numer. Anal. Methods Geomech. 11 (6), 555–583.

Golser, J., 1976. The New Austrian Tunnelling Method (NATM), theoretical background & practical experiences. In: 2nd Shotcrete Conference, Easton, Pennsylvania, USA, October 4–8.

Guan, Z.C., Jiang, Y.J., Tanabashi, Y., 2009. Rheological parameter estimation for the prediction of long-term deformations in conventional tunneling. Tunn. Undergr. Space Technol. 24 (3), 250–259.
Hocking, G., 1976. Three-dimensional elastic stress distribution around the flat end of a cylindrical cavity. Int. J. Rock Mech. Min. Sci. & Geo. Abstr. 13 (12), 331–337.
Hoek, E., 1998. Tunnel support in weak rock. Keynote Address, Symposium of Sedimentary Rock Engineering, Taipei, Taiwan, November 20–22.
Huang, H., Ooka, R., Chen, H., Kato, S., 2009. Optimum design for smoke-control system in buildings considering robustness using CFD and genetic algorithms. Build. Environ. 44 (2009), 2218–2227.
Hudson, J.A., Feng, X.T., 2007. Updated flowcharts for rock mechanics modelling and rock engineering design. Int. J. Rock Mech. Mining Sci. 44 (2), 174–195.
Jiao, Y.Y., Fan, S.C., Zhao, J., 2005. Numerical investigation of joint effect on shock wave propagation in jointed rock masses. J. Test. Eval. 33 (3), 197–203.
Kaiser, P.K., Zou, D., Lang, P.A., 1990. Stress determination by back analysis of excavation induced stress changes-A case study. Rock Mech. Rock Eng. 23 (3), 185–200.
Khamesi, H., Torabi, S.R., Mirzaei-Nasirabad, H., Ghadiri, Z., 2015. Improving the performance of intelligent back analysis for tunneling using optimized fuzzy systems: case study of the Karaj subway line 2 in Iran. J. Comput. Civil Eng. 29 (6), 1–10.
Kolymbas, D., 2005. Tunnelling and Tunnel Mechanics. Springer-Verlag, Berlin, Heidelberg.
Lai, J.X., Mao, S., Qiu, J.L., Fan, H.B., Zhang, Q., Hu, Z.N., Chen, J.X., 2016a. Investigation progresses and applications of fractional derivative model in geotechnical engineering. Math. Probl. Eng. 3, 1–15.
Lai, J.X., Qiu, J.L., Fan, H.B., Zhang, Q., Hu, Z.N., Wang, J.B., Chen, J.X., 2016b. Fiber Bragg grating sensors-based in-situ monitoring and safety assessment of loess tunnel. J Sens. 16, 1–10.
Lee, J., Akutagawa, S., Yokota, Y., Kitagawa, T., Isogai, A., Matsunaga, T., 2006. Estimation of model parameters and ground movement in shallow NATM tunnel by means of neural network. Tunn. Undergr. Space Technol. 21 (3), 242–249.
Li, P.F., Zhao, Y., Liu, J.Y., 2014. Deformation characteristics and control method of tunnel with weak surrounding rock. China Railw. Sci. 35 (5), 55–60.
Li, P.F., Zhao, Y., Zhou, X.J., 2016. Displacement characteristics of high-speed railway tunnel construction in loess ground by using multi-step excavation method. Tunn. Undergr. Space Technol. 51, 41–55.
Li, X.H., Jin, X.G., Kang, H.M., Lu, Y.Y., 2001. Intelligent back analysis of tunnel rock displacement and its application. Chin. J. Undergr. Space Eng. 21 (4), 299–304 (in Chinese).
Liang, Y.C., Feng, D.P., Liu, G.R., Yang, X.W., Han, X., 2003. Neural identification of rock parameters using fuzzy adaptive learning parameters. Comput. Struct. 81 (24), 2373–2382.
Luo, Y.B., Chen, J.X., Huang, P., Tang, M.Q., Qiao, X., Liu, Q., 2017a. Deformation and mechanical model of temporary support sidewall in tunnel cutting partial section. Tunn. Undergr. Space Technol. 61, 40–49.
Luo, Y.B., Chen, J.X., Xi, W.Z., Zhao, P.Y., Li, J.Z., Qiao, X., Liu, Q., 2017b. Application of a total station with RDM to monitor tunnel displacement. ASCE J. Perform. Construct. Facilit. 31 (4), 04017030. http://dx.doi.org/10.1061/(ASCE)CF.1943-5509.0001027.
Luo, Y.B., Chen, J.X., Xi, W.Z., Zhao, P.Y., Qiao, X., Deng, X.H., 2016. Analysis of tunnel displacement accuracy with total station. Measurement 83, 29–37.
Miranda, T., Dias, D., Eclaircy-Caudron, S., et al., 2011. Back analysis of geomechanical parameters by optimisation of a 3D model of an underground structure. Tunn. Undergr. Space Technol. 26 (6), 659–673.
Okabe, T., Hayashi, K., Shinohara, N., Takasugi, S., 1998. Inversion of drilling-induced tensile fracture data obtained from a single inclined borehole. Int. J. Rock Mech. Mining Sci. 35 (6), 747–758.
Ranken, R.E., Ghaboussi, J., 1975. Tunnel design considerations: Analysis of stresses and deformations around advancing tunnels. Final Report to Federal Railroad Administration, Report No. FRAOR & D 75–84, Department of Transportation, Washington, DC.
Ren, G., Smith, J.V., Tang, J.W., Xie, Y.M., 2005. Underground excavation shape optimization using an evolutionary procedure. Comput. Geotech. 32 (2), 122–132.
Sakurai, S., Akutagawa, S., Tokudome, O., 2010. Back analysis of non-elastic strains based on the minimum norm solution. Proc. Japan Soc. Civil Eng. 517, 197–202.
Sakurai, S., Takeuchi, K., 1983. Back analysis of measured displacements of tunnels. Rock Mech. Rock Eng. 16 (3), 173–180.
Schubert, W., Steindorfer, A., Button, A.E., 2002. Displacement monitoring in tunnels - an overview. Felsbau 20 (2), 7–15.
Sharifzadeha, M., Kolivand, F., Ghorbani, M., Yasrobi, S., 2013. Design of sequential excavation method for large span urban tunnels in soft ground-Niayesh tunnel. Tunn. Undergr. Space Technol. 35, 178–188.
Song, S.G., Li, S.C., Li, L.P., Zhang, Q.Q., Wang, K., Zhou, Y., Liu, H.L., 2016. Study on longitudinal deformation profile of rock mass in a subsea tunnel. Mar. Georesour. Geotechnol. 34 (4), 376–383.
Vardakos, S.S., Gutierrez, M.S., Barton, N.R., 2007. Back-analysis of Shimizu tunnel no. 3 by distinct element modeling. Tunn. Undergr. Space Technol. 22 (4), 401–413.
Yang, C.X., Wu, Y.H., Hon, T., 2010. A no-tension elastic–plastic model and optimized back-analysis technique for modeling nonlinear mechanical behavior of rock mass in tunneling. Tunn. Undergr. Space Technol. 25 (2010), 279–289.
Yeh, W.W., Yoon, Y.S., 1981. Aquifer parameter identification with optimum dimension in parameterization. Water Resour. Res. 17 (3), 664–672.
Yin, R.R., Zhu, H.H., 2004. Back-analysis of elastoplastic model of soil. J. Jiangsu Univ. Sci. Technol. (Nat. Sci. Ed.) 18 (03), 21–25 (in Chinese).
Yu, Y.Z., Zhang, B.Y., Yuan, H.N., 2007. An intelligent displacement back analysis method for earth-rockfill dams. Comput. Geotech. 34 (2007), 423–434.
Zhang, D.M., Zhang, C.Y., Zhang, Y., Wang, Y.H., 2011. Back analysis and optimal computation of rock mass in tunnel construction. Chin. J. Undergr. Space Eng. 07 (s2), 1603–1608 (in Chinese).
Zhang, D.L., Fang, Q., Li, P.F., Wong, L.N.Y., 2013. Structural responses of secondary lining of high-speed railway tunnel excavated in loess ground. Adv. Struct. Eng. 16 (8), 1371–1379.
Zhao, Y., 2010. Study on dynamic deformation rules and control technology of surrounding rock for tunnel. J. Beijing Jiaotong Univ. 34 (4), 1–5 (in Chinese).